

## Research papers

## Heat transfer analysis of sewer system and its potential role in thermal energy storage

Chuanyu Zhang<sup>a,b,d</sup>, Xiaofeng Guo<sup>b,c</sup>, Laurent Royon<sup>b</sup>, Patrice Chatellier<sup>a,\*</sup><sup>a</sup> COSYS, Univ Gustave Eiffel, F-77447, Marne-la-Vallée, France<sup>b</sup> Univ Paris Cité, CNRS, LIED UMR8236, F-75006, Paris, France<sup>c</sup> ESIEE Paris, Univ Gustave Eiffel, F-93162, Noisy-le-Grand, France<sup>d</sup> State Key Laboratory for Manufacturing Systems Engineering, Xi'an Jiaotong University, 710049, Xi'an, China

## ARTICLE INFO

## Keywords:

Heat transfer analysis  
Sewer pipe  
Thermal energy storage  
Heating and cooling

## ABSTRACT

Wastewater from urban areas contains a large amount of thermal energy. It constantly exchanges this energy with its surrounding. This study analyzes the thermal exchanges between wastewater and its immediate environment. A mathematical model is constructed that allows to predict the level and velocity of the water in the sewer as a function of time. From this information, the model calculates the heat transfer between the wastewater and the surrounding soil. The results show that the soil temperature can be modified over a maximum thickness of 5 to 10 m. Close to the sewer, soil temperature is constantly influenced by the wastewater, while the soil beyond 10 m does not participate to the exchange. Regarding the heat exchange between wastewater and its environment, the results show that at least 90% of the heat exchange takes place with soil through the part of the pipe in contact with the wastewater while only 10% of the exchange takes place through the air contained in the pipe. The simulations also show the interest of carrying out charge/discharge of thermal energy with the ground surrounding a sewer. For a sewer of 1800 m length and a wastewater flow of 65 m<sup>3</sup>/h during the day and 35 m<sup>3</sup>/h during the night, one can expect to transfer up to 76 kW during the day and discharge 40 kW during the night. In addition, the flow rate plays an important role in the heat transfer process, especially with a partially filled sewer pipe. A higher flow rate means a larger wet area in the pipe and thus an increase in heat exchange. This preliminary analysis shows that the sewer network can be used as an underground thermal storage system to cope with the variations in heating and cooling demand with the goal of improving urban energy efficiency.

## 1. Introduction

The link between extreme weather events and global climate change is becoming increasingly clear. In order to avoid these climate disasters, it is essential to reduce greenhouse gas (GHG) emissions until carbon neutrality is achieved. This objective concerns in particular cities, which account for 70% of the world's energy consumption and the corresponding GHG emissions [1,2]. This share is increasingly high with the global trend towards urbanization. Although the challenge is significant, there are opportunities to decrease the amount of GHG produced by densely populated cities. This is because energy supply and consumption in urban areas is highly centralized, which allows the energy system optimization through a variety of actions. For example, research on smart building envelopes can help reduce heating and cooling needs [3] by adjusting solar gain through variable facade reflectivity. As far as energy production is concerned, heat pumps can be used to recover low quality energy (e.g. thermal energy from air,

water, or waste...) [4,5], or to integrate renewable energy sources (e.g. solar, wind, geothermal...) [6,7]. The implementation of these new generation heating and cooling networks is a critical point in the construction of new districts. These networks operate in a closed circuit with an increasing use of energy recovery at the point of consumption. This is fundamentally different from the conventional network that has an input–output type of operation [8]. In the new network approach, the consumer becomes a *prosumer*, which means that a consumer can also act as a producer. In the coming years, the use of this term is expected to increase in the field of heating and cooling of buildings.

## 1.1. Heating and cooling recovery

Heating and cooling recovery from urban water cycle, including both drinking water and wastewater, represents huge and low-carbon thermal energy sources [1,9]. On the one side, heat recovery from

\* Corresponding author.

E-mail address: [patrice.chatellier@univ-eiffel.fr](mailto:patrice.chatellier@univ-eiffel.fr) (P. Chatellier).

wastewater can provide building heating through a district heating network. On the other, cold recovery from drinking water [10] can increase energy efficiency of cooling units and, together with cold storage, provide electricity savings as well as peak grid demand lowering. In December 2018, wastewater was officially recognized by the European Union as renewable source of energy [11].

As a potential decarbonized source for the next-generation of urban energy configuration, wastewater heat recovery in district heating have been investigated from different perspectives. Hao et al. [12] compared energy recovery potential from wastewater in the form of thermal and chemical energy. The enthalpy-based thermodynamic approach has shown a higher potential for energy recovery from wastewater heat than from the biochemical transformation of organic matter. The chemical energy only accounts for about 10% of the total energy recovery potential, in spite of its high exergy value. Meggers et al. [13] have tried to integrate the heat recovery from hot water just after usage, through a household heat pump. This led to a significant energy demand reduction by comparison to scenarios without this type of recovery. Similarly, Deng et al. [14] have done experiments on the recovering of thermal energy from shower water using heat exchangers. Their results, calculated on the basis of the standard method for evaluating the building energy saving performance (NEN 7120+C2:2012, 2012) show that 61% to 64% and 57% to 62% energy efficiency can be achieved under Winter and Summer conditions respectively. Yet, the above individual systems cannot guarantee the matching between energy demand and recovery supply. In this regard, wastewater heat recovery works better at the district-scale. Guo and Hendel [1] took Paris as an example to assess the heat recovery potential through data from a field-performance monitoring. Their study shows that the recovery system gave up to 75% green gas emission reductions and 30% energy savings. This study obviously proved the significant role played by the heat recovery in urban area. Similarly, van der Hoek et al. [10,15], from TU Delft and Waternet, studied the energy transition of Amsterdam water cycle. They made a feasibility analysis based on economic benefits and potential CO<sub>2</sub> emission reduction by the heat recovery from wastewater. They showed that cold recovery from water mains led to 90% reduction of GHG emissions. Hepbasli et al. [4] comprehensively summarized the studies about Wastewater Source Heat Pump systems in terms of applications and performance assessments. Their review demonstrates that wastewater, as a low-grade heat source, can be utilized in heat pump system and the corresponding systems present higher efficiency and are more environment-friendly.

Another important factor is the energy transport vector for district heating and cooling, in which wastewater energy recovery can be integrated. Spriet et al. [11] attempted spatio-temporal analyses of energy demand and supply. Their results demonstrates the importance of the matching between the wastewater energy recovery and the demand of the energy distribution infrastructure. The upcoming 4th generation of district heating [8] provides opportunities to low-temperature heating. In this regard, the underground wastewater should play a more significant role in the future district heating system. In a more drastic manner, de Chalendar et al. [16] demonstrated a fully integrated electrified heating and cooling network on the campus of Stanford University. The system allows significant reduction in terms of carbon footprint with a particular role of the thermal energy storage elements. Their results showed district-scale thermal storage is critical in a future low carbon city.

### 1.2. Modeling of wastewater dynamics

The characteristics of wastewater depend on human activities and local weather conditions. The variability of these parameters leads to a great fluctuation of wastewater characteristics in terms of flow and temperature which must be taken into account in the wastewater energy recovery processes. As for renewable energy sources, the precise modeling of the energy source is a prerequisite to its integration in an energy

demand management system. Beside experimental studies, researches have been led to build up mathematical models to analyze the dynamic behavior of the underground sewer pipe system. Elías-Maxil et al. [17] built up a model to predict the flow rate at specific positions in the sewer system under different weather conditions. Their study linked a stochastic model for wastewater discharge to Saint-Venant equations or shallow water equation (derived from Navier Stokes equations to describe dynamic state of fluids under shallow water conditions) and achieved validated simulations results. Dürrenmatt et al. [18] have experimentally validated their simulations to predict the evolution of wastewater in terms of temperature and discharge rate. They have developed an open source program, TEMPEST, to facilitate the design of heat recovery from sewer network. The above two simulation studies are focused on the dynamic behavior of the wastewater in the pipe. Meanwhile, important heat exchange can happen between wastewater in sewer and the surrounding soil. Similar to Borehole Thermal Energy Storage (BTES) system, sewer-soil systems can be an easy-to-implement as Thermal Energy Storage (TES) medium. To the best of our knowledge, the analysis of the corresponding energy exchange around the wastewater, including air and soil, is still lacking in the modeling of wastewater dynamics.

In summary, wastewater is discharged from buildings then flows to a WasteWater Treatment Plant (WWTP) through a sewer. Studies has confirmed that thermal energy potential is greater than organic potential through the production of bio-methane [12]. Compared to deploying other costly energy efficiency of renewable energy projects it is worth to use wastewater existing infrastructure in all urban areas by interconnecting buildings. Meanwhile, the thermal energy availability of wastewater is highly influenced by heat losses to air, soil and pipe, and thus is a complex transient phenomenon.

In this study, we construct a dynamic model considering the evolution of wastewater flow and the radial heat transfer along a sewer pipe. The study is focused on the coupling of energy transfer between wastewater, sewer and soil, including the air contained in the sewer.

The paper is organized as follows. First, a mathematical model is built and validated to describe the dynamic state of wastewater. The heat exchange between soil and sewer pipe along the radial direction of the pipe is taken into account. Then, results are analyzed to answer the question whether the soil surrounding the pipe has a potential role as thermal storage medium to buffer the variations of wastewater. Then the influence of soil thickness and inlet conditions on the energy storage function are discussed. Finally, perspectives are given to shed light on plausible application of sewer pipe system to the future's energy system.

## 2. Theoretical model

A general hydro-thermal model of a sewer partially filled of wastewater, based on the work of Dürrenmatt et al. [18,19], is shown in Fig. 1. This model handles sewer pipes located at several meters below the surface. Given this depth constraint, we have assumed that the influences of ground level temperature and geothermal energy can be neglected.

The modeling process includes three steps: (i) calculation of the wastewater flow in the sewer, (ii) modeling of air flow, including air temperature and humidity, (iii) modeling sensible heat transfer between wastewater, pipe and soil and latent transfer between wastewater and air. Each of these processes is described separately in the following sub-sections. Specifically, the model takes into account the inlet flowrate and temperature. For the modeling, we firstly solve the one dimensional Saint-Venant equations (with respect to  $x$ ) to determine the height of water along the pipe. Then the temperature of wastewater and air in the headspace are solved. A radial symmetry condition is assumed for the heat transfer between wastewater and pipe, and between pipe and soil. This means that the heat transfer in pipe and soil along tangent direction is neglected.

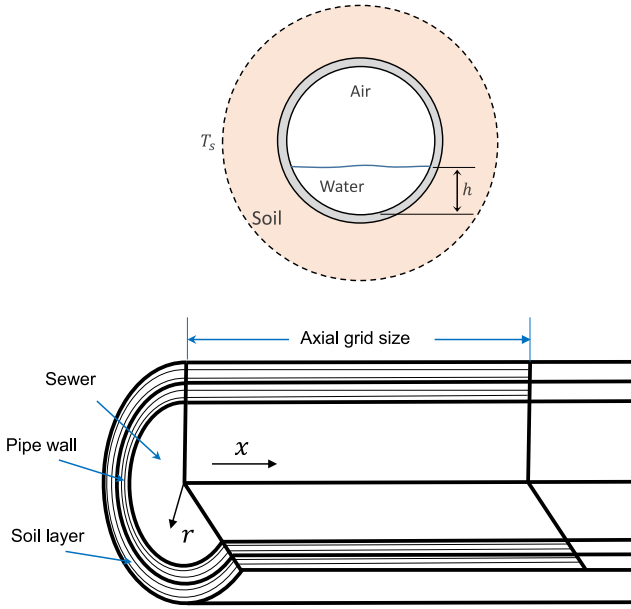


Fig. 1. General schematic of the hydro-thermal model of a sewer system.

#### Dynamic state of wastewater

One dimensional Saint Venant equations are used to describe the dynamic behavior of the wastewater flow in a partially filled sewer:

$$\frac{\partial h}{\partial t} + \frac{A_w}{b} * \frac{V}{x} + V * \frac{\partial h}{\partial x} + \frac{V}{b} * \left( \frac{\partial A_w}{\partial x} \right)_{h=\text{constant}} + J_{ecw} * P / (\rho_w * b) = 0 \quad (1)$$

$$\frac{\partial V}{\partial t} + V * \frac{\partial V}{\partial x} + g * \frac{\partial h}{\partial x} + g * (S_f - S_0) = 0 \quad (2)$$

Here  $h$ ,  $A_w$ ,  $V$ ,  $\rho_w$  refer to the height, wet cross-section area, velocity and density of wastewater;  $b = \partial A_w / \partial h$  refers to the free surface width in the pipe;  $S_f$  and  $S_0$  are designated as friction sloop and channel bottom sloop respectively, particularly the sloop rate  $S_f$  is necessary to overcome the frictional resistance in a steady flow by gravity. In this study, the cross section along the flow direction is uniform and so  $\frac{\partial A_w}{\partial x} = 0$ .  $J_{ecw}$  is the mass flux due to evaporation or condensation between water and air in the headspace of the pipe. Its expression is given in Table 3 of Appendix.  $P$  is the wet perimeter.

#### Airflow in the headspace

In this study, it is assumed that pressure equilibrium of air between inlet and outlet is constantly satisfied. So the airflow in the headspace is only caused by the variations of wastewater depth. The mass balance of the airflow  $Q_a$  in the headspace per unit of sewer is given by:

$$\frac{\partial A_a}{\partial t} + \frac{\partial Q_a}{\partial x} = 0 \quad (3)$$

where  $A_a$  is the cross-sectional area of the air headspace,  $A_a = A - A_w$ . According to Eq. (3), the  $Q_a$  can be obtained by integrating of cross-sectional area of wastewater starting from the inlet:

$$Q_a(t, x) = \int_0^x \frac{\partial A_w(t, x)}{\partial t} dx + Q_{a0} \quad (4)$$

Here the  $Q_{a0}$  is the steady term of  $Q_a$  and can be evaluated with the expression by Edwini-Bonsu et al. [20] and David.J et al. [18]

$$Q_{a0} = \frac{0.856}{L} \int_0^L A_a V_{w,s} \frac{P}{U_a + P} dx \quad (5)$$

Details about the determination of  $V_{w,s}$  in a circular conduit is given in Appendix.

#### Temperature and humidity

Vapor load  $X$  per mass unit of dry air, air temperature  $T_a$  in the headspace and wastewater temperature  $T_w$  are given by:

$$\frac{\partial A_a X}{\partial t} + \frac{\partial (V A_a X)}{\partial x} = \frac{1}{\rho_a} * (J_{ec} * P - J_{cp} * U_a - J'_{ca} * A_a) \quad (6)$$

$$\frac{\partial A_a T_a}{\partial t} + \frac{\partial (V A_a T_a)}{\partial x} = \frac{1}{c_a * \rho_a} * (q_{pa} U_a + q_{wa} * P + q'_{ca} A_a) \quad (7)$$

$$\frac{\partial A_w T_w}{\partial t} + \frac{\partial (V A_w T_w)}{\partial x} = \frac{1}{c_w \rho_w} (q_{pw} U_w - q_{wa} P - q_{ecw} P + q'_{COD} A_w) \quad (8)$$

The meanings of  $P$ ,  $U$ ,  $A$  are given in Table 3 of Appendix.  $q_{pw}$  is the heat transfer rate per unit area between wastewater and pipe.

#### Heat transfer in pipe and soil

Temperatures  $T_p(x, r, t)$  and  $T_s(x, r, t)$  in the pipe and in the soil are given by :

$$\frac{\partial T_p}{\partial t} + \nabla \cdot \left( -\frac{k_p}{\rho_p c_p} \nabla T_p \right) = \frac{1}{\rho_p c_p} q_{pw} \quad (9)$$

$$\frac{\partial T_s}{\partial t} + \nabla \cdot \left( -\frac{k_s}{\rho_s c_s} \nabla T_s \right) = \frac{1}{\rho_s c_s} q_{ps} \quad (10)$$

Where,  $q_{ps}$  is the heat transfer rate at the interface between soil and pipe.

#### Boundary conditions

The height of the wastewater at the inlet is required for solving the dynamic state equations Eqs. (1) and (2):

$$h(x = 0, t) = h(t) \quad (11)$$

For the heat and humidity equations Eqs. (6), (7) and (8), Dirichlet boundary conditions at the inlet are required:

$$T_w(x = 0, t) = T_w(t); T_a(x = 0, t) = T_a(t); X(x = 0, t) = X(t) \quad (12)$$

For the heat transfer equations in pipe and soil (Eqs. (9) and (10)) Neumann conditions are required.

At the interface between wastewater and pipe wall this boundary condition is written as:

$$\lambda_p \frac{\partial T_{pw}(t, r = D/2, x)}{\partial r} = k_{pw}(T_{pw} - T_w) \quad (13)$$

At the interface between air and pipe wall the boundary condition is defined as:

$$\lambda_p \frac{\partial T_{pa}(t, r = D/2, x)}{\partial r} = k_{pa}(T_{pa} - T_w) - q_{cp} \quad (14)$$

At the interface between pipe wall and soil the boundary condition is defined as:

$$\lambda_p \frac{\partial T_s(t, r = D/2 + s, x)}{\partial r} = \lambda_s \frac{\partial T_p(t, r = D/2 + s, x)}{\partial r} \quad (15)$$

In these equations,  $T_w$  is the wastewater inlet temperature,  $T_{pw}$  (resp.  $T_{pa}$ ) is the temperature at the interface between pipe wall and wastewater (resp. between pipe wall and air),  $\lambda_{ps}$  (resp.  $\lambda_s$ ) is the heat conductivity of the pipe (resp. soil) and  $s$  is the wall thickness.

The outer boundary condition of the soil layer is Dirichlet condition at the interface between disturbed and undisturbed soil

$$T_s(t, r = D/2 + s + \delta_s, x) = T_{s,\infty} \quad (16)$$

The value of  $\delta_s$  is the thickness of soil layer surrounding the sewer pipe where the temperature is disturbed by the sewer pipe. Let us remind that we assumed the top of the sewer pipe lays at a depth of several meters from the ground surface. For soil and wastewater the boundary conditions depends on  $T_{s,\infty}$ ,  $T_w$  and  $T_{pw}$  which are different under winter conditions as shown in Table 1. The data are retrieved from Chalhoub et al. [21] who conducted on-field soil temperature measurement at different depths in the region of Paris, France.

**Table 1**

Winter boundary conditions for soil and wastewater. \* means that the variable is not involved in the specific condition; - indicates that the variable is not constant in the specific condition.

	$T_{s,\infty}$	Initial conditions	inlet $T_w$	$T_{pw}$
		Steady solution	*	13 °C
Winter	5.5 °C	IC1(as Fig. 5(a))	13 °C - 3 °C/ + 2 °C	-
		IC2(as Fig. 5(b))	13 °C	-

**Initial conditions**

Due to soil thermal inertia, once deeper soil layer is involved, initial conditions could significantly affect the results. Specifically, for a soil layer of 10 m. One way to set up the initial conditions is to use steady solution of Eqs. (9) and (10) (i.e. assuming  $\partial T/\partial t$  is equal to zero in both equations). This assumes that the boundary conditions at the water side  $T_w$  and at the soil side  $T_{s,\infty}$  keep constant for several years which may not be realistic for on-site applications.

Therefore in this study we have chosen to test three possible initial conditions for winter:

1. Steady solution with constant boundary conditions: 13 °C for  $T_{pw}$  and 5.5 °C for  $T_{s,\infty}$ . Here, the analytical solution of Eq. (10) ( $\partial T/\partial t = 0$ ) for temperature profile in soil is introduced.
2. Initial condition 1 (IC1): A daily cycle of 2 °C above and 3 °C below 13 °C for the inlet temperature is added to the undisturbed pipe and soil temperature and lasts for one month (720 h), as shown Fig. 5(a). The temperature profile along  $r$  direction after one month is shown in Fig. 5(c).
3. Initial condition 2 (IC2): A constant temperature of 13 °C is set as inlet temperature for one month, as shown in Fig. 5(b). The corresponding temperature profile along  $r$  direction after one month is plotted in Fig. 5(c).

In addition, it should be noted that spatial IC1 and IC2 for pipe and soil are established with simulation from an initial constant temperature of 5.5 °C of water, pipe wall and soil. In the following, the expression “initial conditions” specifically refers to IC1 and IC2.

**Time step and grid cell size**

Different grid sizes are adopted to discretize the domain in axial and radial directions. For the radial direction, as we will discuss in Section 3, based on the semi-analytical solution Eq. (17), the transfer rate of the characteristic physical information (the temperature in this study), namely the time needed to transfer the temperature between consecutive nodes within the radial grid is much larger than the time step  $\Delta t_s$  adopted. Then no special limit on the radial grid size ( $\Delta r$ ) is necessary and the grid size is set to  $s/4$  in the pipe wall and to  $\delta_s/10$  in the soil.

The variation of water temperature along the flow (axial) direction is used as a criterion to verify the proper choice of time step  $t_s$  and grid size in the axial direction ( $g_x$ ). The temperature trend should not contain drastic shift in a very short distance or a brief time step. The trade-off is to satisfy CFL stability conditions while maintaining an acceptable computing load. In this study, we associate  $t_s = 2$  s with  $g_x = 10$  m in all studied cases. This choice gives accurate simulation for reasonable computational efforts. The details of the grid refinements study are given in Appendix through Figs. 12 and 13.

The temperature and mass variations Eqs. (1)–(8) are solved with commercial software COMSOL Multiphysics [22] based on the module “General form PDE(g)”, while the heat transfer process in the pipe and soil (Eqs. (9)–(10)) are simulated by module “Heat transfer in Solids(ht)”.

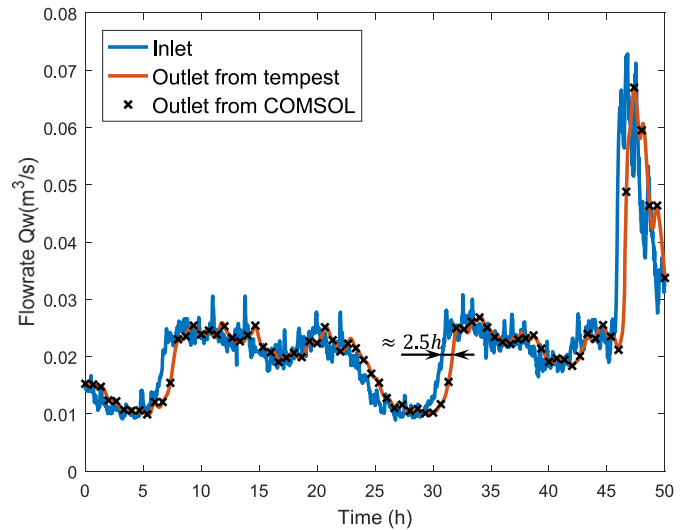


Fig. 2. Evolution of wastewater flowrate  $Q_w$ , in  $m^3/s$ , from discharge to the outlet. The dynamic response delay from inlet to outlet is about 1 h~3 h, depending on the specific flowrate at the inlet.

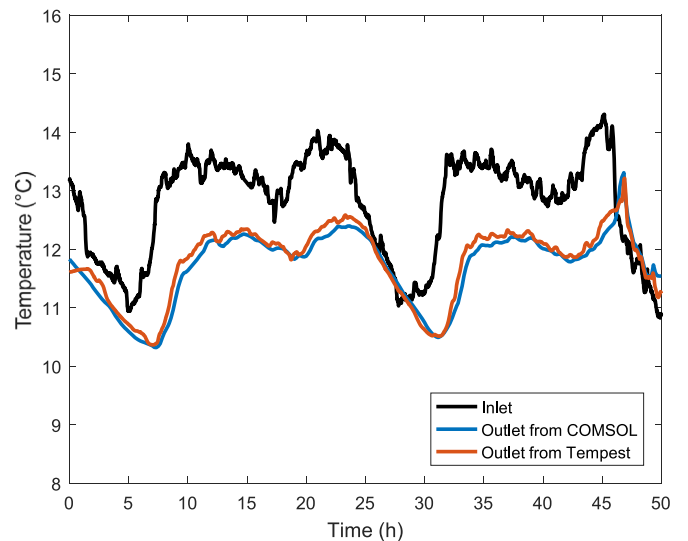


Fig. 3. Evolution of wastewater temperature from discharge to outlet.

**3. Validation of the model**

*Validation with experimental results*

The COMSOL model has been validated with regard to TEMPEST by comparing the values obtained for the wastewater temperature  $T_w$  and the flowrate at the outlet  $Q_w$ . The validation of TEMPEST data has been completed by Dürrenmatt et al. [18] through on-field experimental studies. The data of flowrate and temperature at the inlet from TEMPEST were measured in a section of the sewer between Rüläng and Oberglatt in the Canton of Zurich, Switzerland [18].

In Figs. 2 and 3, we compare flowrate evolution during 48 h as well as the inlet/outlet temperature distribution during the same period of time. It appears clearly that, with the same  $Q_w$  and  $T_w$ , the values given by COMSOL and TEMPEST overlap. This result shows that the COMSOL model can be used to deeply investigate the system.

One particular characteristic of the sewer system is the time shift between inlet and outlet in terms of temperature and flow rate. Indeed, according to inlet (discharge) flow rate, evolution at the outlet can

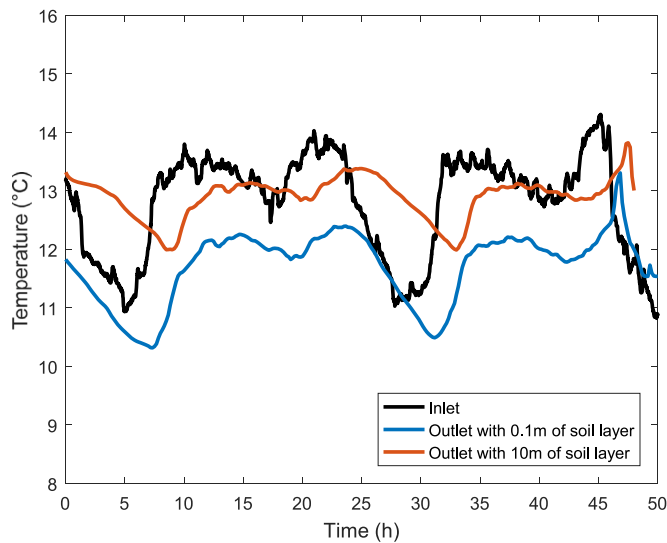


Fig. 4. Evolution of wastewater temperature from discharge to the outlet, with 0.1 m and 10 m soil layers.

be delayed by about 1 to 3 h (Fig. 2). In addition to time delay, temperature evolution with time (Fig. 3) has smaller amplitude at the outlet than at the inlet. This is due to the thermal inertia of pipe-soil system. These features are different from most conventional thermal systems and can be potentially used for Thermal Energy Storage (TES) applications.

Finally, let us note that the validations are made with the same soil depth ( $\delta_s = 0.1$  m) as in the case studied in TEMPEST [18]. This means it is assumed that for soil area deeper than 0.1 m from the sewer, the temperature is no longer influenced by the wastewater in the pipe. Beside, following the procedure of TEMPEST, a steady solution is achieved and taken as the initial condition for later dynamic calculation. However, this procedure might bring problems when the thickness of soil layer is large and the heat capacity of the soil part cannot be neglected. As shown in Fig. 4, when the depth of the soil involved in the model is changed from 0.1 m to 10 m, the temperature at the outlet shows significant differences, at least within the first hours (Fig. 4 shows a 50 h calculation period). Although these differences seem to be diminishing as the calculation period prolongs (period from 45 h to the end), it makes the depth of the soil around the sewer and the corresponding initial conditions emerge as prominent factors, especially when we try to introduce a sharp change of energy input or output to the water, as in the strategies used in the studies concerning TES.

#### Influence of initial conditions and soil depth

As discussed above, when deeper soil layer is involved, the initial conditions influence the whole system and changes the outlet temperature, in particular at the beginning of operating period. Using the three initial conditions, i.e. IC1 (Fig. 5(a)), IC2 (Fig. 5(b)) and steady solution (analytical solution, Fig. 5(c)) of the temperature profile described above, the corresponding radial soil temperature profiles are plotted in Fig. 5(c). We notice very close profiles for conditions IC1 and IC2 while these curves are still far from the steady state one. The role played by such differences on the following study depends on the duration of the simulated period as shown in Fig. 6. Here we impose the same daily temperature cycle as IC1 after each of the three initial conditions. Results in terms of outlet temperature show clear differences during the first several days, but these differences no longer exist after ten days. This indicates the soil-pipe system requires long enough operating time to remove the influence of initial conditions. As the focus of our study is

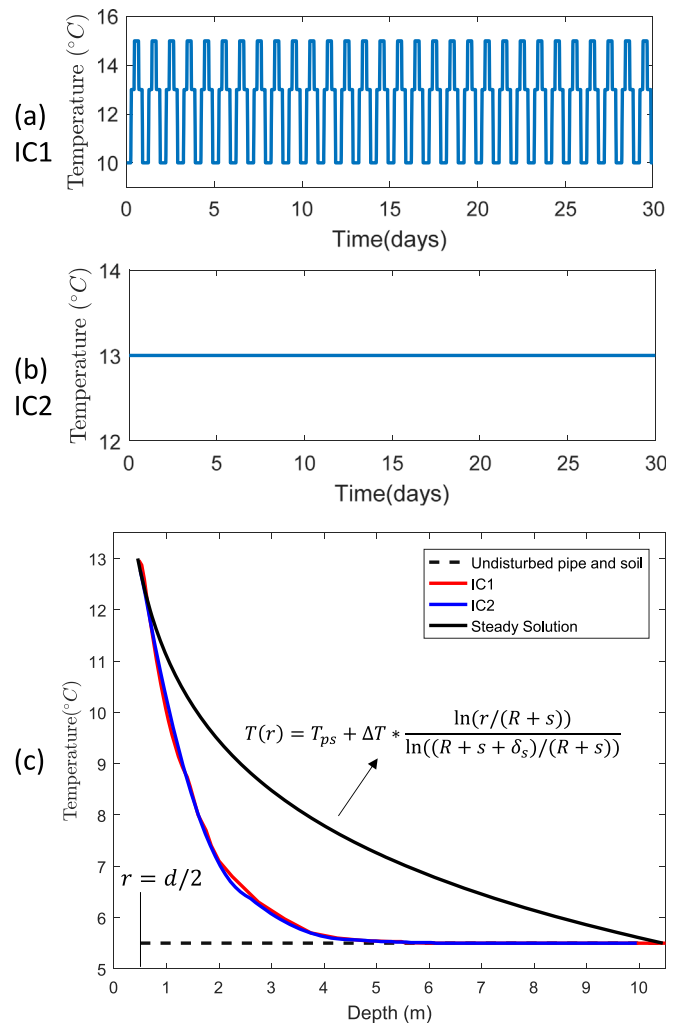


Fig. 5. The variations of inlet temperature for Initial Condition 1 (a) and Initial Condition 2 (b); and their corresponding temperature profile along  $r$  direction in (c).  $\Delta T$  is temperature difference between wastewater and undisturbed soil, here  $\Delta T = 7.5$  °C.

hourly to daily TES applications, we should carefully define appropriate initial conditions upon which all our conclusions are based.

In addition, the soil thickness ( $\delta_s$ ) involved in the heat transfer with the sewer is another important parameter. As a typical transient heat conduction phenomenon, the influential thickness depends on soil properties and time duration. To approximate the soil thickness that must be taken into account by the model, we use the classical transient analytical solution of heat transfer in semi-infinite case:

$$\frac{T(x, t) - T_i}{T_s - T_i} = 1 - \text{erf}\left(\frac{x}{2\sqrt{at}}\right) \quad (17)$$

where  $T(x, t)$  refers to temperature at distance  $x$  from the pipe wall and at time  $t$ .  $T_i$  is the initial temperature of the whole domain while  $T_s$  is the shock temperature at the surface  $x = 0$  and  $\alpha$  the thermal diffusivity.

In our case, we assume a quasi-steady situation when the ratio  $(T(x, t) - T_i)/(T_s - T_i)$  is less or equal to 1%, i.e. at time  $t$ , soil beyond  $x$  is no longer influenced by the surface boundary condition  $T_s$ .

As the  $\alpha_{concrete}$  is greater than  $\alpha_{soil}$ , a value of  $\alpha$  equal to  $\alpha_{soil}$  is adopted in order to find the smallest value of  $x$  above which equilibrium is reached. For most wastewater dynamic studies focusing on sub-hourly flow-temperature evolution, one can assume the duration of 1 h characterizes the dynamics of the inlet temperature. In this case, assuming  $\alpha = \alpha_{soil} = 0.5 \times 10^{-6}$  m<sup>2</sup>/s, Eq. (17) states that  $x$  must be greater than 0,154 m in order to reach the equilibrium. Accordingly,

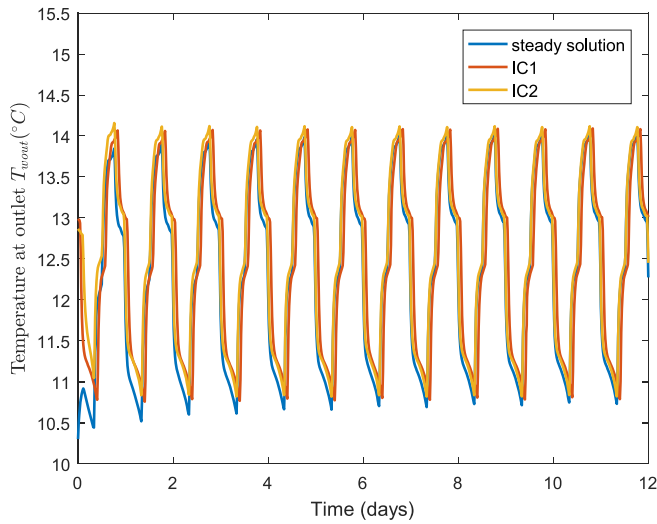


Fig. 6. The evolution of outlet temperature based on three different initial conditions: Steady solution, IC1 and IC2.

the depth should satisfy  $x \leq 1$  m and  $x \leq 10$  m for  $t = 1$  h and  $t = 4286$  h respectively.

Studying hourly or daily thermal energy storage requires hourly or daily temperature variation conditions. In Fig. 7(a), an artificial evolution of inlet temperature  $T_w$  is introduced to show the influence of a sharp change of  $T_w$  on the heat flux at different depths of soil below the pipe wall. Here, we assume that a sharp decrease of inlet  $T_w$  happens during the initial 2 h, then  $T_w$  remains constant at 11 °C. Fig. 7(b) represents the variations of heat flux along  $z$  direction per meter of pipe ( $q$ ) with the distance below the pipe wall at 1 h (i.e. when  $T_w$  is changing at the inlet) and 2160 h (i.e. a long enough time after the change of  $T_w$  allowing us to assume that the steady state is reached). From the profile of  $q$ , we can conclude the heat flux through the soil at 10 m or deeper approaches zero and is not influenced by the variations of wastewater temperature for a period as long as 3 months. We thus choose to model  $x = 10$  m of soil depth below the pipe wall which can cover both short and long terms cases. Nevertheless, for most hourly TES scenarios, heat flow from or to the wastewater only happens within a much thinner soil layer. This will be discussed later.

#### 4. Results and discussions

Before presenting the results, let us define several parameters used later:

1.  $q_{pwx} = q_{pw} * U_w$ , heat transfer rate between wastewater and pipe per unit length along  $x$  direction (flow direction);
2.  $q_w = q_{pw}U_w - q_{wa}P - q_{ecw}P + q'_{COD}A_w$ , the energy variation rate of water per unit length along  $x$  direction. In the following we assume  $q'_{COD}A_w = 0$ ;
3.  $q_{tot} = \int_0^L q_{pwx}dx$ , the total heat transfer rate throughout pipe, and  $q_{l_1l_2} = \int_{l_1}^{l_2} q_{pwx}dx$  the total heat transfer rate from  $l_1$  to  $l_2$ ;
4.  $q_{sx}$ , the heat transfer rate per unit of length along  $x$  direction at a certain depth below the pipe

##### Division of heat dissipation

Firstly, we aim to quantify how thermal energy is dissipated from wastewater to its surrounding environment, i.e. air and soil. Fig. 8 shows the proportion of  $q_{pwx}$  to  $q_w$  in the situation shown in Fig. 4. The ratio keeps above 90% most of the time. This indicates that, the  $q_{pwx}$  dominates the evolution of energy of wastewater, and other energy

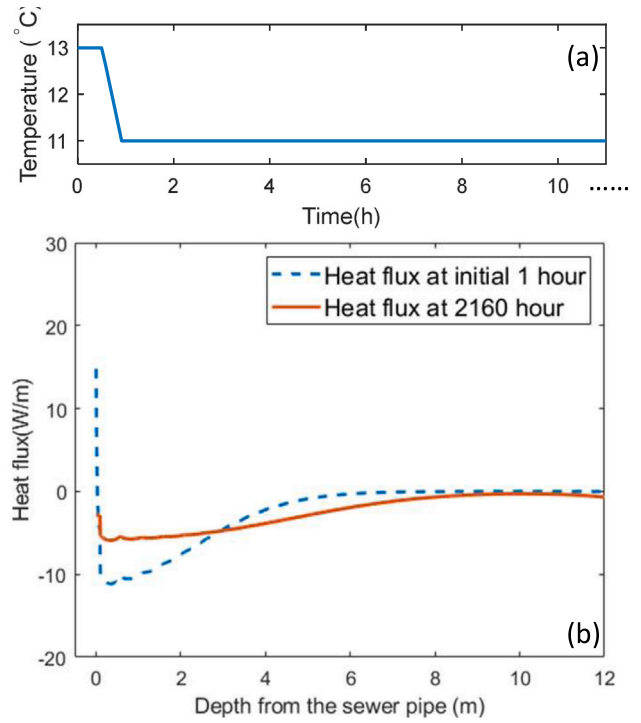


Fig. 7. (a) Time variation of the temperature at the pipe inlet. (b) Heat transfer rate  $q$  at one hour (i.e. just before the temperature changes) and 2160 h (i.e. as a function of depth when steady state is assumed to be reached).

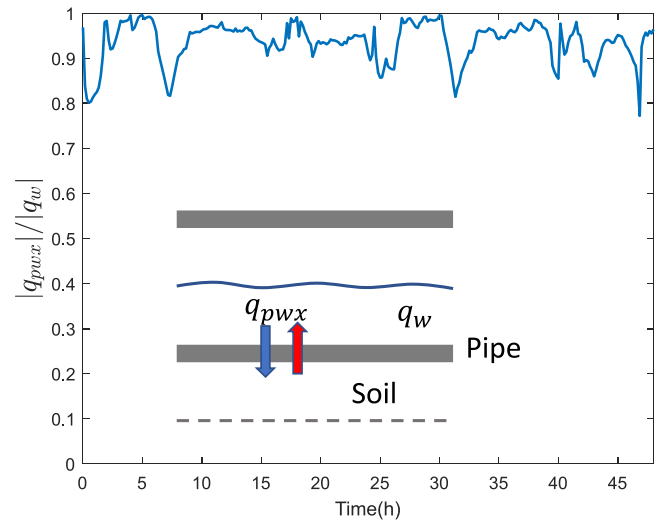


Fig. 8. The ratio of heat flux between wastewater and pipe  $q_{pwx}$  to the total energy variation of wastewater  $q_w$ .

terms like heat transfer from wastewater to air can be neglected. So it is reasonable to pay most of our attention to heat transfer between wastewater and pipe when trying to interpret the variation of energy of wastewater in the pipe.

##### TES charging and discharging

In the following, we discuss the feasibility of achieving TES, first following protocols of charging and discharging, as shown in Fig. 5(a) ( $\Delta T = +2$  °C during daytime and  $\Delta T = -3$  °C during night), second setting 13 °C as inlet temperature.

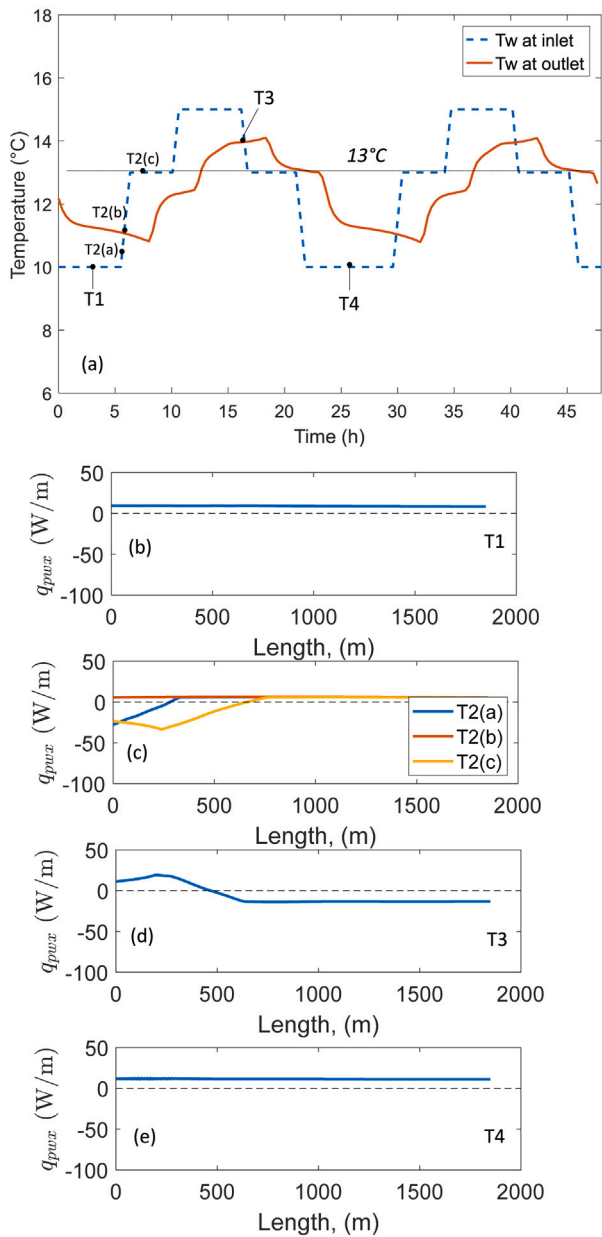


Fig. 9. TES functionality. (a) Charging/discharging profiles following a +2/−3 °C protocol based on the bench temperature of 13 °C. (b)–(e) Heat flux per unit length along the flow direction at several times. The corresponding time points (T1~T4) are marked in (a).

As shown in Fig. 9, within 48 h of winter condition, we have considered an undisturbed soil temperature of 6° [21], and a variable temperature at the inlet. Here we use 13 °C as the bench value for wastewater temperature at the inlet. During the night, i.e. from 0 to 6 h, 22 h to 28 h and 46 h to 48 h,  $T_w$  at the inlet remains at low value (10 °C) and collects the heat energy from the pipe and soil, while it remains at 15 °C during daytime and charges the pipe and soil with energy. From the perspective of  $T_w$  at the outlet, the value keeps correlated to the inlet value during the initial period (T1, limited by the initialization), then as  $T_w$  increases at inlet (T2(a), T2(b), T2(c) and T3), it varies correspondingly but keeps lower than the inlet value. During this process, heat is continuously transferred from water to the pipe then to the soil (thermal charge phase). The crossover between these

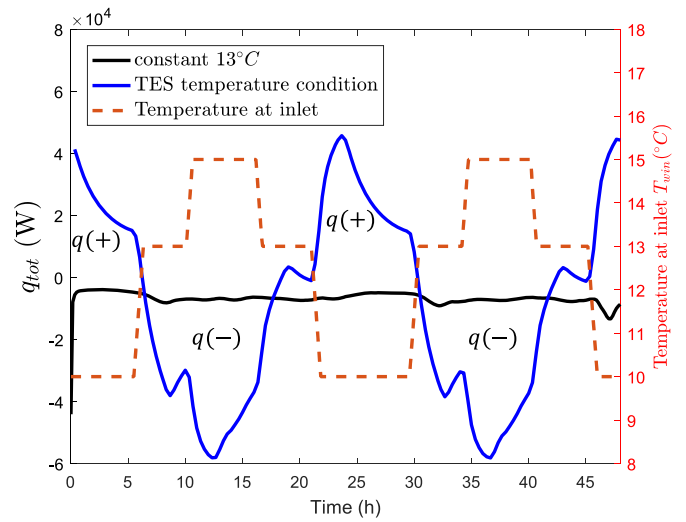


Fig. 10. TES functionality: total heat transfer rate in different situations. The black curve gives the heat flux when  $T_w$  at the inlet keeps constant at 13 °C. It refers to the left y axis. Curves blue and dashed red refer to periodic variations of  $T_w$  as in Fig. 9(a). Blue curve refers to the left y axis while dashed red curve refers to the right y axis. (For interpretation of the references to color in this figure legend, the reader is referred to the web version of this article.)

two temperatures happens at T3, which means the start of the energy discharge to wastewater from the pipe (thermal discharge phase). This energy collection lasts until a new increase of inlet temperature.

The evolution of heat flux  $q_{pwx}$  from T1 to T4 is shown in the sub figures of Fig. 9. During the charge phase (T2 to T3),  $q_{pwx}$  remains negative while it keeps positive during the discharge phase (T3 to T4). The dynamic of  $q_{pwx}$  evolution along the axial length is also shown in these figures, especially in the sub-figure showing T2. From T2(a) to T2(c), as more wastewater with higher temperature flows into the sewer, larger  $q_{pwx}$  extends along length from the inlet until the turning point appears when the  $T_w$  at the inlet no longer increases and keeps constant at 13 °C.

#### Total heat flux during the charging and discharging process

As defined above  $q_{tot}$  is the heat flux between the wastewater and pipe integrated along the whole length of the pipe. In Fig. 10, dynamic variations of  $q_{tot}$  are plotted under two situations: (i)  $T_w$  at the inlet keeps equal to 13 °C; (ii)  $T_w$  at the inlet has the same profile as in Fig. 9. Fig. 10 shows that, in the first case, the total heat flux changes a little with time but remains close to zero indicating that the steady state is quite reached. In the second situation, when the periodically variable temperature is set at the inlet, significant variations of the total heat flux between negative and positive value appear. This means that the heat exchange between wastewater and pipe is bidirectional. These variations closely correspond to the changes of the temperature at the inlet. An increase of  $T_w$  at the inlet causes a decreasing total heat flux while a positive value comes up after a lasting decrease of  $T_w$ . Besides, the highest values of 59 kW and 41 kW can be reached respectively during charging and discharging period.

#### The distribution of heat flux along pipe

Fig. 11 shows the evolution of the heat flux  $q_{pwx}$  with time for three different positions in the pipe : the inlet, the middle and the outlet. Like the total heat flux  $q_{tot}$ , the local heat flux  $q_{pwx}$  also oscillates between negative and positive values, although there is a clear lag for the variations at middle position (925 m) and outlet (1850 m). Meanwhile, it can be seen that the maximum values during the charging

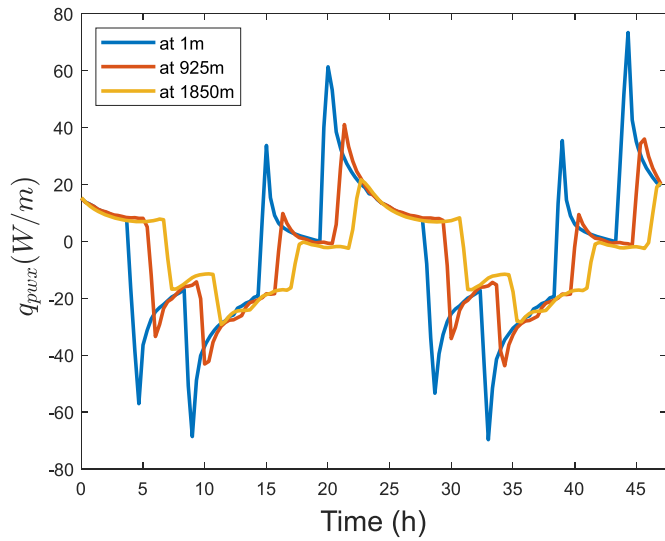


Fig. 11. Heat flux at the interface between wastewater and pipe wall at different locations in the pipe.

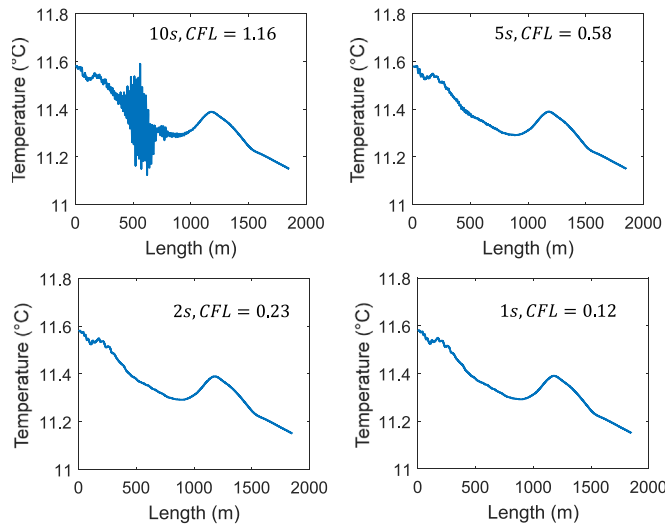


Fig. 12. The variations of temperature along flow direction with different time steps  $t_s$ :  $t = 190$  min,  $g_x = 10$  m,  $CFL = (V^*t_s/g_x)$  is the Courant Number.

or discharging process decrease along the pipe, varying from 70 W/m at 1 m to 30 W/m at 1850 m. This means that density of heat flux decays along the flow direction and so does the heat storage capacity. This is because the maximum temperature difference between wastewater and pipe always appears at the inlet. In terms of application, it appears that the recovery equipment should be mounted near the wastewater inlet to the sewer in order to collect more energy.

### 5. Concluding remarks

In this study, we build up a dynamic model of the interactions between wastewater, sewer and soil. This model was used for sewer pipes located at several meters below the surface where the influences of ground level temperature and geothermal energy can be neglected. This model was developed in COMSOL and validated by results previously reported by TEMPEST. The tool was used to investigate the dynamic variations of wastewater flow rate and temperature in a sewer pipe and its heat exchange with the surrounding environment.

The main conclusions are the following:

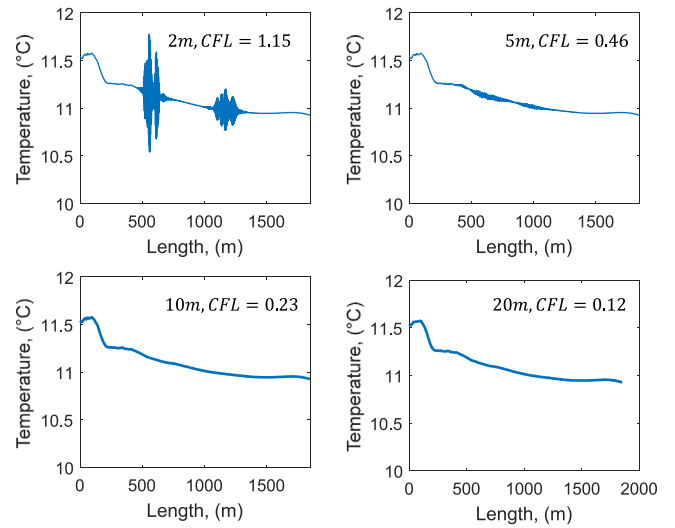


Fig. 13. The temperature along flow direction with different  $g_x$ :  $t = 210$  min,  $t_s = 2$  s.

Table 2

The values of constant parameters in the model from Eqs. (3) to (10).

Symbol	Meaning	Values
$\rho_a$	Density of air above the water	1.19 [kg/m <sup>3</sup> ]
$c_a$	Heat capacity of air	1007 [J/(kg K)]
$c_w$	Heat capacity of water	4181 [J/(kg K)]
$c_p$	Heat capacity of pipe	690 [J/(kg K)]
$c_s$	Heat capacity of soil	559 [J/(kg K)]
$\rho_w$	Density of water	998.2 [kg/m <sup>3</sup> ]
$\rho_p$	Density of pipe	2300 [kg/m <sup>3</sup> ]
$\rho_s$	Density of soil	1500 [kg/m <sup>3</sup> ]
$\lambda_p$	Heat conductivity of pipe	$1 \times 10^{-6}$ [m <sup>2</sup> /s]
$\lambda_s$	Heat conductivity of soil	$0.2 \times 10^{-6}$ [m <sup>2</sup> /s]

1. Heat transfer depth in soil: the thickness of the soil layer taken into account greatly influences the solution in terms of heat transfer process. In the current study, 10 m is considered as an optimal thickness.
2. Ninety percent of heat is dissipated through the wet part of the pipe instead of air in the head.
3. Sewer can play an important role in TES: We have studied an example of infrastructure and flow rate and have shown that realistic temperature variations at the input allow heat charging and discharging with the ground. Preliminary values of 76 kW and 40 kW can be reached respectively for charging and discharging.
4. Flow rate plays an important role on the heat transfer process in partially filled sewer pipes as higher flow rate means larger wet area leading to an increase of heat exchanges.
5. Regarding the TES functionality, the study unveils the importance of initial conditions before implementing heat/cold storage. A proper measurement of the vertical soil temperature distribution, for a depth as high as 10 m is necessary to establish the most realistic underground temperature profile as initial conditions.

Our ongoing studies are focused on the coupling of sewer with a renewable thermal plant (like solar energy) to quantify the role of sewer on TES. Besides, an optimal control strategy of charging/discharging can be searched with the developed model. Another area of work could

**Table 3**

Nomenclature in the model from Eqs. (3) to (10) and the their corresponding expressions. It should be noted that the  $P$ ,  $U$ ,  $A$  are achieved by fitting curves with respect to the height  $h$  of the wastewater. This function is completed through module of "Variable Definition/Interpolation" in COMSOL.

Symbol	Meaning	Expressions
$P$	Width of water level(m)	$P = f(h)$ (Fitting curve)
$U$	Perimeter	$U = f(h)$ (Fitting curve)
$A$	Cross-sectional area	$A = f(h)$ (Fitting curve)
$D$	Nominal diameter of the sewer pipe	0.9 m
$V_{w,s}$	Wastewater velocity at the surface	$V_w + \frac{V_w^2}{0.4} (\frac{3}{2} + 2.3 \log \frac{2h'}{D})$ $V_w^* = \sqrt{g R_{w,hy} S_0}$ , $h' = h$ if $h \leq D/2$ or $h' = D - h$
$p_{sat}(T)$	saturation partial pressure at temperature $T$	$p_{sat}(T) = p_{so} e^{-\frac{T_0}{T}}$
$j_{ecw}$	Mass flux during evaporation or condensation	$j_{ecw} = \alpha_{ecw} (p_{sat}(T_w - p_a)) / h_{fg}$
$\alpha_{ecw}$	Mass transfer coefficient	$\alpha_{ecw} = 8.75 \sqrt{ V_w - V_a }$ (W/m <sup>2</sup> /mbar)
$h_{fg}$	enthalpy of evaporation	$h_{fg} = 2.45 \times 10^6$ (J/kg)
$j_{cp}$	Mass flux of condensation on pipe	$j_{cp} = q_{cp} / h_{fg}$
$q_{cp}$	Heat flux of condensation on pipe	$q_{cp} = 0$ when $p_a(T_a) < p_{sat}(T_{pa})$ or $q_{cp} = \alpha_{cp} (p_a - p_{sat}(T_{pa}))$ when $p_a(T_a) \geq p_{sat}(T_{pa})$
$\alpha_{cp}$	Coefficient of heat transfer of condensation on pipe	$\alpha_{cp} = 8.75 \sqrt{ V_a }$ (W/m <sup>2</sup> /mbar)
$j'_{ca}$	Mass flux of condensation in air	$j'_{ca} = 0$ when $X < X_{sat}$ or $j'_{ca} = \rho_a (X - X_{sat}) / t_s$ when $X \geq X_{sat}$
$q_{pa}$	Heat flux between headspace air and pipe	$q_{pa} = \alpha_{pa} (T_{pa} - T_a)$
$\alpha_{pa}$	heat transfer coefficient with respect to hydrodynamic state	$\alpha_{pa} = \frac{0.023 Re_w^{1/5} Pr_w^{1/3} \lambda_a}{R_{w,hy}}$ ( $Re_w \geq 10000$ and $0.7 \leq Pr_w \leq 160$ )
$T_{pa}$	pipe temperature at the interface between pipe wall and air	Initial value is given
$q_{wa}$	Heat flux between water and air	$q_{wa} = \alpha_{wa} (T_w - T_a)$
$\alpha_{wa}$	heat transfer coefficient of $q_{wa}$	$\alpha_{wa} = 5.85 \sqrt{ V_a - V_w }$ (W/m <sup>2</sup> /K)
$q'_{ca}$	Heat flux during condensation or evaporation process	$q'_{ca} = 0$ when $X(T_a) < X_{sat}(T_a)$ or $q'_{ca} = h_{fg} j'_{ca}$ when $X(T_a) \geq X_{sat}(T_a)$
$q_{pw}$	Heat flux between water and pipe	$q_{pw} = k_{pw} (T_{pw} - T_w)$
$k_{pw}$	heat transfer coefficient of $q_{pw}$	$k_{pw} = 1 / (1/\alpha_{pw} + 1/f)$
$1/f$	heat transfer resistance by biofilm growth on the pipe wall	0.005(m <sup>2</sup> K/W)
$\alpha_{pw}$	heat transfer coefficient with respect to hydrodynamic state	$\alpha_{pw} = \frac{0.023 Re_w^{1/5} Pr_w^{1/3} \lambda_w}{R_{w,hy}}$ ( $Re_w \geq 10000$ and $0.7 \leq Pr_w \leq 160$ )
$T_{pw}$	pipe temperature at the interface between pipe wall and water	Initial value is given
$q_{ecw}$	Heat flux of evaporation and condensation	$q_{ecw} = \alpha_{ecw} (P_{sat}(T_w - P_a))$
$q'_{cod}$	Heat produced during bio-degradation	$q_{cod} = e_{cod} r_{cod}$
$e_{cod}$	enthalpy of bio-degradation reaction	$e_{cod} = 1.4 \times 10^7$ (J/kg)
$r_{cod}$	degradation rate	$r_{cod} = 2.8 \times 10^{-6}$ (kg/m <sup>3</sup> /s)
$q_{ps}$	Heat flux between pipe and soil	

be to improve the model to make it capable of taking into account the long-term, seasonal variation of the temperature at the surface of the ground as well as the influence of the geothermal energy. These improvements will require the development of a truly 3D model.

### CRediT authorship contribution statement

**Chuanyu Zhang:** Investigation, Software, Writing – review & editing. **Xiaofeng Guo:** Funding acquisition, Supervision, Writing – review & editing. **Laurent Royon:** Review. **Patrice Chatellier:** Funding acquisition, Supervision, Review.

### Data availability

Data will be made available on request.

### Acknowledgments

This study has received supports from the I-SITE FUTURE, a government grant managed by the Agence Nationale de la Recherche, France

under the Investissements d'avenir program (ANR-16-IDEX-0003) in addition to the contributions of the institutions involved.

### Appendix

#### Time step and grid size verification

Figs. 12 and 13 present the variation of temperature along flow direction (axial direction) with different time steps  $t_s$  and  $g_x$ . By comparison, when the  $t_s > 2$  s or  $g_x < 10$  m, drastic variations without physical meaning appear around some grid points. In this situation, the local velocity  $V' = V + \sqrt{gh}$  is comparable or larger than the characteristic time of the model  $V^* = \Delta x / \Delta t$  and accuracy of the solution cannot be assured. So in this study, in order to optimize the computation load, we chosen for all the studied cases a time step  $t_s$  of 2 s associated to a space discretization of  $g_x = 10$  m.

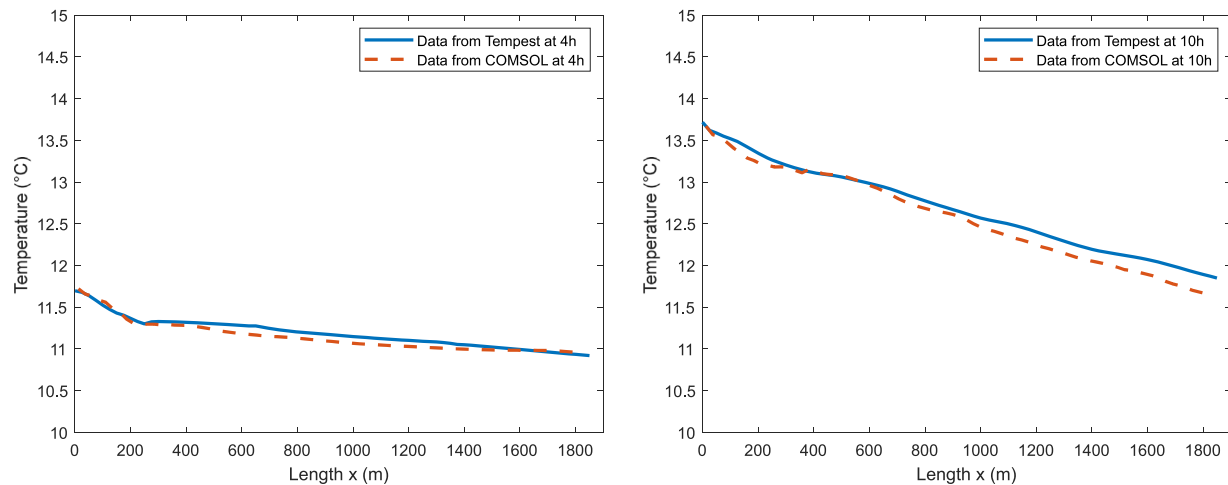


Fig. 14. Comparison in terms of wastewater temperature from TEMPEST and Comsol at 4 h and 10 h.

#### Validation with TEMPEST regarding spatial temperature distribution

We also compare the  $x$ -direction temperature profiles obtained by our COMSOL model against TEMPEST results. Fig. 14 shows these profiles at 4 h and 10 h with the same initial conditions as Fig. 3.

Similar to Fig. 3, the spatial results show good agreement at both 4 h and 10 h from the beginning, considering the whole length of the sewer pipe (1850 m).

#### Constant parameters

The following symbols and abbreviations are used in the study (see Table 2).

#### Nomenclature

The following symbols and abbreviations are used in the study (see Table 3).

#### References

- [1] X. Guo, M. Hendel, Urban water networks as an alternative source for district heating and emergency heat-wave cooling, *Energy* 145 (2018) 79–87, <http://dx.doi.org/10.1016/j.energy.2017.12.108>.
- [2] P. Droege (Ed.), *Urban Energy Transition - 2nd Edition*, Elsevier, 2018, p. 706, URL <https://www.elsevier.com/books/urban-energy-transition/droege/978-0-08-102074-6>.
- [3] C. Wang, Y. Zhu, X. Guo, Thermally responsive coating on building heating and cooling energy efficiency and indoor comfort improvement, *Appl. Energy* 253 (June) (2019) 113506, <http://dx.doi.org/10.1016/j.apenergy.2019.113506>.
- [4] A. Hepbasli, E. Biyik, O. Ekren, H. Gunerhan, M. Araz, A key review of wastewater source heat pump (WWSHP) systems, *Energy Convers. Manage.* 88 (2014) 700–722, <http://dx.doi.org/10.1016/j.enconman.2014.08.065>.
- [5] A. Mehari, Z.Y. Xu, R.Z. Wang, Thermal energy storage using absorption cycle and system: A comprehensive review, *Energy Convers. Manage.* 206 (December 2019) (2020) <http://dx.doi.org/10.1016/j.enconman.2020.112482>.
- [6] N.M. Haegel, H. Atwater, T. Barnes, C. Breyer, A. Burrell, Y.-M. Chiang, S. De Wolf, B. Dimmler, D. Feldman, S. Glunz, J.C. Goldschmidt, D. Hochschild, R. Inzunza, I. Kaizuka, B. Kroposki, S. Kurtz, S. Leu, R. Margolis, K. Matsubara, A. Metz, W.K. Metzger, M. Morjaria, S. Niki, S. Nowak, I.M. Peters, S. Philipps, T. Reindl, A. Richter, D. Rose, K. Sakurai, R. Schlatmann, M. Shikano, W. Sinke, R. Sinton, B. Stanbery, M. Topic, W. Tumas, Y. Ueda, J. van de Lagemaat, P. Verlinden, M. Vetter, E. Warren, M. Werner, M. Yamaguchi, A.W. Bett, Terawatt-scale photovoltaics: Transform global energy, *Science* 364 (6443) (2019) 836–838, <http://dx.doi.org/10.1126/science.aaw1845>.
- [7] J.F. Manwell, J.G. McGowan, A.L. Rogers, *Wind Energy Explained Theory, Design and Application Second Edition*, 2009.
- [8] M. Sulzer, S. Werner, S. Mennel, M. Wetter, Smart Energy Vocabulary for the fourth generation of district heating and cooling, *Smart Energy* 1 (2021) 100003, <http://dx.doi.org/10.1016/j.segy.2021.100003>.
- [9] S. Lyu, C. Wang, C. Zhang, L. Royon, X. Guo, Experimental characterization of a novel soft polymer heat exchanger for wastewater heat recovery, *Int. J. Heat Mass Transfer* 161 (2020) <http://dx.doi.org/10.1016/j.ijheatmasstransfer.2020.120256>.
- [10] J.P.V.D. Hoek, S. Mol, S. Giorgi, J.I. Ahmad, Energy recovery from the water cycle: Thermal energy from drinking water, *Energy* (2018) <http://dx.doi.org/10.1016/j.energy.2018.08.097>.
- [11] J. Spriet, A. McNabola, G. Neugebauer, G. Stoeglehner, F. Kretschmer, J. Spriet, A. McNabola, G. Neugebauer, G. Stoeglehner, T. Ertl, Spatial and temporal considerations in the performance of wastewater heat recovery systems, *J. Clean. Prod.* (2019) <http://dx.doi.org/10.1016/j.jclepro.2019.119583>.
- [12] X. Hao, J. Li, M.C.M.V. Loosdrecht, H. Jiang, R. Liu, Energy recovery from wastewater : Heat over organics 161, 2019, pp. 2011–2014, <http://dx.doi.org/10.1016/j.watres.2019.05.106>.
- [13] F. Meggers, H. Leibundgut, The potential of wastewater heat and exergy : Decentralized high-temperature recovery with a heat pump, *Energy Build.* 43 (4) (2011) 879–886, <http://dx.doi.org/10.1016/j.enbuild.2010.12.008>.
- [14] Z.S.M. Deng, J.P. van der Hoek, Shower heat exchanger : Reuse of energy from heated drinking water for CO 2 reduction, 2016, pp. 1–8, <http://dx.doi.org/10.5194/dwes-9-1-2016>.
- [15] V.D. Hoek, J. Peter, J. Imtiaz, V.D. Hoek, G.T. Energy, D. Water, I.J. Kroppe, A.G. Olabi, D. Goricanec, S.B. Eds, Delft University of Technology thermal energy recovery from drinking water, 2017, <http://dx.doi.org/10.18690/978-961>.
- [16] J.A.D. Chalendar, W. Glynn, S.M. Benson, Environmental Science integrated energy systems †, 2019, <http://dx.doi.org/10.1039/c8ee03706j>.
- [17] J.A. Elías-Maxil, J. Hofman, B. Wols, F. Clemens, J.P. van der Hoek, L. Rietveld, Development and performance of a parsimonious model to estimate temperature in sewer networks, *Urban Water J.* 14 (8) (2017) 829–838, <http://dx.doi.org/10.1080/1573062X.2016.1276811>.
- [18] D.J. Dürrenmatt, O. Wanner, A mathematical model to predict the effect of heat recovery on the wastewater temperature in sewers, *Water Res.* 48 (1) (2014) 548–558, <http://dx.doi.org/10.1016/j.watres.2013.10.017>.
- [19] D.J. Dürrenmatt, O. Wanner, *Computer program for the simulation of the wastewater temperature in sewers*, 2008.
- [20] S. Edwini-Bonsu, P.M. Steffler, Air flow in sanitary sewer conduits due to wastewater drag: A computational fluid dynamics approach, *J. Environ. Eng. Sci.* 3 (5) (2004) 331–342, <http://dx.doi.org/10.1139/S03-072>.
- [21] M. Chalhoub, M. Bernier, Y. Coquet, M. Philippe, A simple heat and moisture transfer model to predict ground temperature for shallow ground heat exchangers, *Renew. Energy* 103 (2017) 295–307, <http://dx.doi.org/10.1016/j.renene.2016.11.027>.
- [22] C. Multiphysics, *Introduction to COMSOL multiphysics®*, 1998, p. 2018, COMSOL Multiphysics, Burlington, MA, Accessed Feb 9.